PNAS RESEARCH ARTICLE | NEUROSCIENCE OPEN ACCESS

Endogenous circadian reporters reveal functional differences of *PERIOD* paralogs and the significance of PERIOD:CK1 stable interaction

Jiyoung Park[a], Kwangjun Lee[a], Hyeongseok Kim[b], Heungsop Shin[b], and Choogon Lee[a,1]

Edited by Joseph Takahashi, The University of Texas Southwestern Medical Center, Dallas, TX; received July 17, 2022; accepted December 22, 2022

Adverse consequences from having a faulty circadian clock include compromised sleep quality and poor performance in the short-term, and metabolic diseases and cancer in the long-term. However, our understanding of circadian disorders is limited by the incompleteness of our molecular models and our dearth of defined mutant models. Because it would be prohibitively expensive to develop live animal models to study the full range of complicated clock mechanisms, we developed *PER1-luc* and *PER2-luc* endogenous circadian reporters in a validated clock cell model, U-2 OS, where the genome can be easily manipulated, and functional consequences of mutations can be accurately studied. When major clock genes were knocked out in these cells, circadian rhythms were modulated similarly compared with corresponding mutant mice, validating the platform for genetics studies. Using these reporter cells, we uncovered critical differences between two paralogs of *PER*. Although *PER1* and *PER2* are considered redundant and either one can serve as a pacemaker alone, they were dramatically different in biochemical parameters such as stability and phosphorylation kinetics. Consistently, circadian phase was dramatically different between *PER1* and *PER2* knockout reporter cells. We further showed that the stable binding of casein kinase1δ/ε to PER is not required for PER phosphorylation itself, but is critical for delayed timing of phosphorylation. Our system can be used as an efficient platform to study circadian disorders associated with pathogenic mutations and their underlying molecular mechanisms.

circadian | reporter | crispr | period | bioluminescence

Significance

Genetic and environmental disruption to the circadian clock can lead to diverse diseases including sleep and metabolic disorders. Cells with engineered circadian reporters, especially bioluminescence reporters, have been instrumental in understanding the mechanisms underpinning circadian rhythms and circadian disorders, but have been limited by the lack of endogenous circadian reporters available for human cells. To address this gap, we have developed two endogenous reporter lines in the human clock cell model, U-2 OS. Using these reporters combined with genome editing by CRISPR, we uncovered how the circadian clock is uniquely regulated in peripheral cells compared with the master clock in the brain. Our cell-based platform will accelerate and enable expanded testing of many mutations in clock genes and mechanistic studies.

The circadian clock drives daily rhythms in behavior and physiology (1–5), and dysfunction or disruption of the clock has been implicated in diverse disease states including sleep disorders (6–10). Decades of prior work have revealed that the clock is built on a core transcriptional feedback loop that is cell autonomous, involving transcriptional and post-translational regulation of the pacemaker *PERIOD* (*PER*) genes (11, 12). In the feedback loop, the activator complex CLOCK:BMAL1 drives transcription of the pacemaker genes *PER1* and *PER2* (*PER*) along with many other clock-controlled genes (ccgs). PER proteins form an inhibitory complex that also contains CRYPTOCHROME (CRY) proteins and casein kinase CK1δ/ε proteins. The circadian phase, e.g., onset of activity or sleep, is determined by the oscillations of this PER/CRY/CK1 complex (13–15).

The paralogs of *PER* and *CRY* genes share some common/redundant functions but also differ in function and regulation. In the case of *PER*, the paralogs *PER1* and *PER2* (*PER3* is considered nonessential) seem to play redundant roles in the master clock tissue, the supraChiasmatic nuclei (SCN), as knockouts (KOs) of either gene produce little period and phase alterations in behavioral rhythms (16, 17). However, the regulation of *PER1* and *PER2* may differ dramatically in peripheral tissues and cell culture. For example, *PER1* transcription in cultured cells is rapidly induced by high serum and forskolin, but *PER2* transcription is marginally affected by these signals (18). In mouse tissues, phases of *PER1* transcript and protein rhythms are advanced relative to those of *PER2* (19). Therefore, the circadian period and phase of PER protein oscillations in *PER1* KO cells and *PER2* KO cells may differ significantly, likely because of different kinetics in messenger RNA (mRNA) and protein profiles in these peripheral cells. This is an unexplored critical issue because circadian properties such as phase of all ccgs can be affected when only one *PER* is present compared with Wild-type (wt) cells. In the case of *CRY,* KOs of *CRY1*, *CRY2,* and *CRY1/2* exhibit shortened rhythms, lengthened rhythms, and arrhythmicity, respectively. Although it has been suggested that difference in binding affinity of two CRYs to CLOCK:BMAL1 is the molecular underpinning for the opposite period alteration in *CRY* single KOs (20, 21), it has not been studied how two CRYs differentially affect the pacemaker genes *PER1* and *PER2*. Period alteration in *CRY* KOs would be manifested ultimately through altered regulation of *PER* at transcriptional and posttranscriptional levels (Table 1).

Author contributions: J.P. and C.L. designed research; J.P., K.L., and C.L. performed research; H.K. and H.S. contributed new reagents/analytic tools; J.P., K.L., and C.L. analyzed data; and J.P., K.L., and C.L. wrote the paper.

The authors declare no competing interest.

This article is a PNAS Direct Submission.

[1]To whom correspondence may be addressed. Email: Choogon.lee@med.fsu.edu.

This article contains supporting information online at https://www.pnas.org/lookup/suppl/doi:10.1073/pnas.2212255120/-/DCSupplemental.

Published February 1, 2023.

Another critical issue in the field is how PER phosphorylation by CK1δ and CK1ε can be extended to over ~12 h, which is responsible for the prolonged circadian feedback loop. This is an unconventional kinase-phosphorylation relationship, especially considering that PER and CK1 make an unusually stable interaction through a dedicated domain in PER called CKBD (Casein Kinase Binding Domain) (19, 22, 23). A series of phosphorylation steps across several serine residues in this domain seems to play an important role in tuning phase and period (21, 24, 25). The Ser662Gly mutation in the CKBD of *PER2* gene causes advanced phase and shortened period in humans, leading to a condition called Familial Advanced Sleep Phase Syndrome (FASPS) (14). Although the FASPS motif has been a main focus of studies of the CKBD due to its defined role in the human sleep disorder, CKBD has other conserved motifs, and it has not been studied how these motifs contribute to the phosphorylation-mediated timing system.

Because the circadian clock is cell autonomous, genetic disruptions of the clock manifest similar phenotypes at the behavioral and cellular levels, and cell culture has proven to be a valuable and valid platform for characterizing the molecular biology of circadian rhythms (13, 26, 27). The endogenous clocks of cultured cells—including mouse embryonic fibroblasts (MEFs) and human U-2 OS (U2OS) cells—can be precisely measured in real time by introducing a luciferase (Luc) reporter gene under control of a clock promoter (26–29). Across numerous studies, such cells have served as functional models for in vivo circadian clocks, and results have been consistently validated in live animal models. Cell culture models are not only less resource-consuming, but also more easily manipulated by chemicals and transgenes, which makes the cell models more suitable for mechanistic studies. One key limitation in cell models today is the lack of endogenous phase and period reporters other than the *mPer2-Luc* reporter in MEFs (26), which is a mouse, not a human cell model. Exogenously transfected reporters like *Per2*- or *Bmal1*-promoter controlled Luc are useful to an extent but do not accurately reflect the endogenous status of the clock.

In this study, we generated human *PER1-luc* and *PER2-luc* endogenous knockin (KI) genes in U2OS cells, to produce a human cell model with robust bioluminescence rhythms. When KO phenotypes for major clock genes were quantified by bioluminescence rhythms in these cells, they were consistent with phenotypes of KO mice. We further used these cells to uncover differences between the paralogs of *PER* and *CRY*, and to gain critical insights into how timing cues are precisely generated by the phosphotimer through dynamic interaction between PER and CK1δ/ε.

Results

Generation of U2OS Cells with Endogenous *PER1-luc* and *PER2-luc* KI Genes and Robust Rhythms in Bioluminescence and Clock Proteins. The main challenge in developing reporter KIs was that the screening process could be very cumbersome due to a high number of off-target insertions (30, 31). We have tested several established protocols employing high-fidelity CAS9 and the paired Cas9D10A nickase approach to decrease off-target insertions (32–34), but they all produced different off-target insertions and offered no meaningful advantage over wtCAS9 for on-target KI generation. To streamline the selection process for positive clones after single-cell sorting, we employed a dual reporter system that eliminates the need for molecular experiments during the selection process (Fig. 1*A*). To generate *PER1* and *PER2* reporter lines, U2OS cells were transfected with two plasmids, all-in-one green fluorescence protein (GFP)-sgRNA-CAS9 (35) and repair templates with Luc-T2A-mRuby3 (Fig. 1*A*). If targeting is successful, Luc-T2A-mRuby3 will be inserted between the last amino acid (AA) and stop codon in each *PER* gene (Fig. 1*A*). The T2A cleavage site was added because Luc alone has been proven not to disrupt PER function or clock function in the $mPer2^{Luc}$ KI mouse (26), whereas this has not been proven for the bulkier Luc-mRuby3 dual tag. In the first selection after transfection, stable mRuby3-expressing cells were singly sorted into 96-well plates by fluorescence-activated cell sorting (FACS). Because we hypothesized mRuby3 expression would be low based on prior work with the *mPer2-GFP* KI mouse (36), we selected a low range of red signal (Fig. 1*B*) for single-cell sorting; this tunability is a major advantage of FACS versus antibiotic selection. Subsequent bioluminescence selection allowed us to select clones with robust rhythms without the need for expansion, genomic DNA prep, and PCR analysis from individual clones (Fig. 1*C*). We isolated 7 final clones for *PER1* (4 hetero- and 3 homozygous (Ho) KIs), and 6 final clones for *PER2* (all heterozygotes). The second selection produced ~30% rhythmic clones. These final clones were further validated by junction PCR and sequencing (Fig. 1*D* and *SI Appendix*, Fig. S1), and by immunoblotting with anti-PER and Luc antibodies (Fig. 1*E* and *SI Appendix*, Fig. S2). Finally, single specific insertions were verified by showing a complete loss of bioluminescence and mRuby3 signals when frame-shifting mutations were introduced in early exons in *PER* genes (*SI Appendix*, Fig. S3).

We confirmed that the KIs did not cause any disruption in clock function by comparing the molecular rhythms between PER and PER-Luc proteins in heterozygote clones (Fig. 2). When comparing *PER1* and *PER2* heterozygote KI clones (hereafter referred to as $PER1^{Luc}$ and $PER2^{Luc}$) (Fig. 2*A*), PER1-Luc peaked 2 to 3 h earlier than PER2-Luc, which is consistent with the phases of PER rhythms in mouse peripheral tissues (19). PER1-Luc signals were higher than those of PER2-Luc reporters (Fig. 2*A* and *SI Appendix*, Fig. S4 *A* and *B*). When these PER^{Luc} reporters were compared with the transgenic *BMAL11-Luc* reporter (27), they showed almost antiphase oscillations, consistent with the natural antiphase oscillations of *PER* vs. *BMAL1* mRNA in vivo (Fig. 2*B*). The periods of *PER1* and *PER2* KI reporters were not different from each other (Fig. 2*C* and *SI Appendix*, Fig. S4*C*), but they were slightly different from that of the transgenic *BMAL1-Luc* reporter. The mouse endogenous $mPer2^{Luc}$ reporter in MEFs produced similarly antiphase oscillations compared with the *BMAL1-Luc* reporter in U2OS cells (Fig. 2*D*). Both PER1-Luc and PER2-Luc fusion proteins showed similarly robust oscillations in abundance and phosphorylation as their wt counterparts in the heterozygote clones (Fig. 2 *E* and *F*). Robust oscillations of PER-Luc fusion proteins were also confirmed by immunoblotting with anti-Luc antibody (Fig. 2 *E*–*G*). The majority of the mobility shift of both PER and PER-Luc was due to phosphorylation (Fig. 2*H*). Finally, their functionality was verified by confirming that PER-Luc-containing clock complexes exhibited the same abundance and phosphorylation rhythms as their wt PER-containing counterparts (Fig. 3*A*).

We have previously shown that the level of PER phosphorylation highly correlates with the size of clock protein complexes because PER hyperphosphorylation is induced by multimerization of PER monomers (37). Studying our PER reporter cells uncovered interesting differences between PER1 and PER2 at the posttranslational level. Although both PER1 and PER2 are much less stable than other clock proteins (38), PER2 was significantly more unstable than PER1 (Fig. 3 *B* and *C*). This was verified by immunoblotting of time course samples and real-time bioluminescence (Fig. 3*C*). More significantly, regarding the phosphotimer function of PER, PER1's progressive phosphorylation occurred significantly

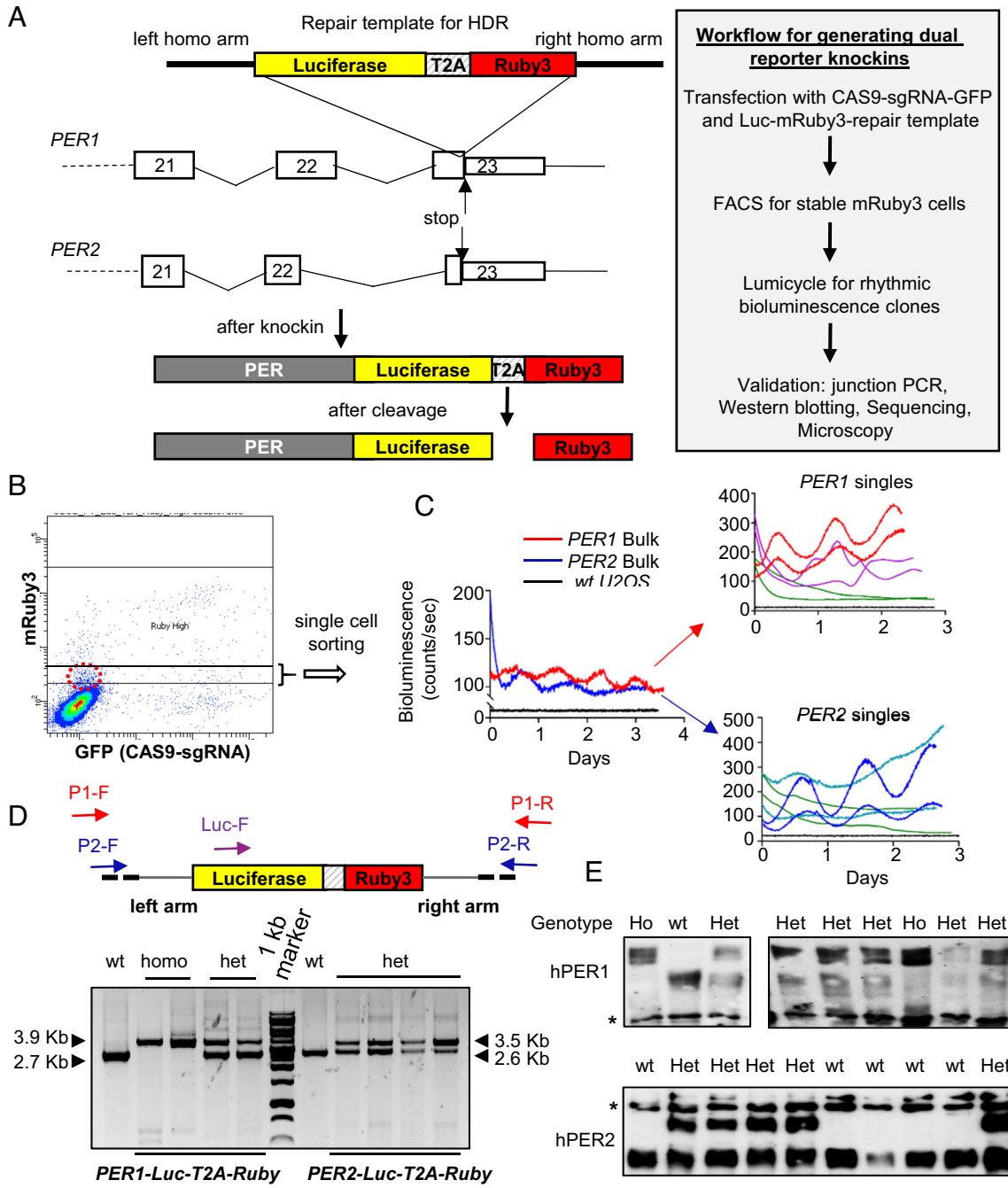

Fig. 1. A streamlined selection process using a tandem reporter system successfully and rapidly identified KI reporter cells. (*A*) KI schematics using a tandem reporter, fluorescence, plus bioluminescence. In heterozygote KI clones, the non-KI alleles had minor mutations near the stop codon due to indels without KI (*SI Appendix*, Fig. S1). (*B*) Cells expressing mRuby3 in a low range were selected in bulk and singly sorted into 96-well plates by FACS. (*C*) The bulk sorted cells and single clones were set up in Lumicycle 96. Note that red and blue traces represent specific $PER1^{Luc}$ and $PER2^{Luc}$ KI clones, respectively. (*D*) Three-primer PCR using two primers binding outside of the homologous arms and a primer binding to Luc was done to screen for on-target KI. (*E*) On-target KI (Ho = homozygous, Het = heterozygous) was confirmed by immunoblotting using anti-PER and anti-Luc antibodies (*SI Appendix*, Fig. S2). * non-specific band.

faster than that of PER2 (Fig. 3*D*). PER1 accumulated faster than PER2 after existing proteins were depleted by a long cycloheximide treatment because PER1 was more stable (Fig. 3*D* and *SI Appendix*, Fig. S5*A*). These data have important implications when either *PER1* or *PER2* is inactivated because although either one can sustain the clock as the sole pacemaker, the resulting oscillations could be very different due to their differences in these key parameters.

Phase of Circadian Genes Is Reversed in *PER1* KO Cells. Numerous lines of evidence indicate that the phases of circadian behaviors such as wake and sleep timing (activity onset and offset) are determined by phases of PER oscillations. For example, new wake/sleep cycles following transmeridian travel are established by altered phases of *PER* genes through realigning of *PER* oscillations to the altered light cycles (1, 39, 40). *PER* genes are the only clock genes that can be phase-shifted directly by light in the SCN. We measured how period and phase of *PER1* and *PER2* genes are affected in nonlight-responsive peripheral clock cells (U2OS) by examining PER-Luc rhythms when the other paralog is absent. When *PER2* was knocked out in $PER1^{Luc}$ cells (Fig. 4 *A*, *B*, and *D*), the period and phase of PER1-Luc rhythms were little changed. However, when *PER1* was knocked out in $PER2^{Luc}$ cells (Fig. 4 *A*, *C*, and *D*), the

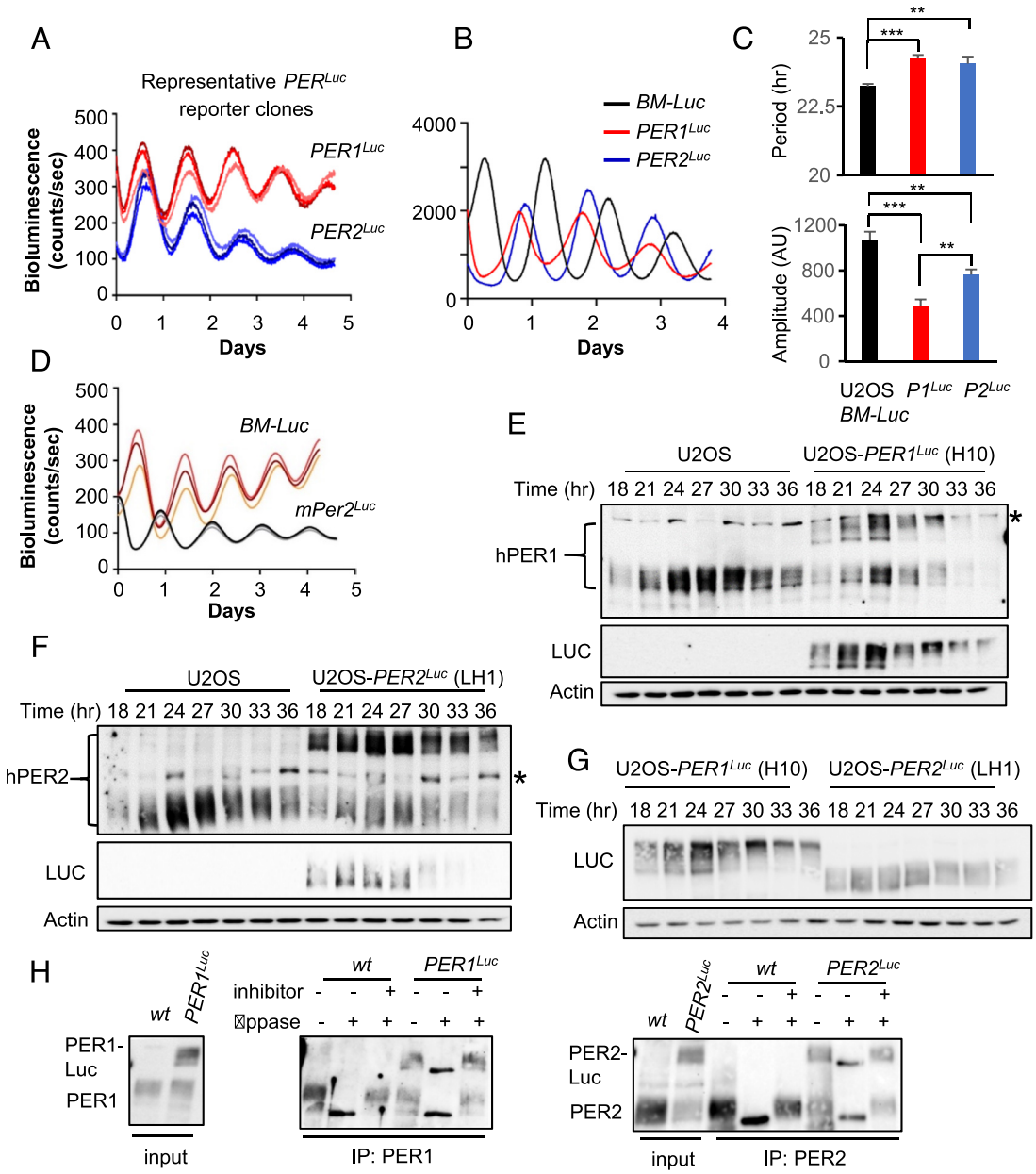

Fig. 2. Endogenous *PER*^{Luc} reporters exhibit robust oscillations without disrupting the clock mechanisms. (*A*) Bioluminescence rhythms are shown for representative Het *PER1*^{Luc} and *PER2*^{Luc} clones, using a similar number of cells. Note that PER1-Luc peaks earlier than PER2-Luc. Three replicates are shown for each clone. Ho *PER1*^{Luc} clones showed higher signals than Het clones demonstrating that reporter cells are highly quantitative (*SI Appendix*, Fig. S4*A*). More clones are shown in *SI Appendix*, Fig. S4 *B* and *C*. (*B*) *PER1*^{Luc} and *PER2*^{Luc} exhibited antiphase oscillations to transgenic *BMAL1* promoter-Luc reporter in U2OS cells. (*C*) Circadian period of *PER1*^{Luc} and *PER2*^{Luc} reporters is not significantly different. Representative of three experiments. Mean ± SD (n = 3, two-tailed *t* test). *<0.05; **<0.01; ***<0.001. (*D*) m*Per2*^{Luc} MEFs showed antiphase oscillations to *BMAL1-Luc* U2OS cells. (*E*–*G*) PER-Luc fusion proteins showed robust oscillations in abundance and phosphorylation almost identical to their wt counterparts. Heterozygote clones, H10 for *PER1*^{Luc} and LH1 for *PER2*^{Luc} were used. See *SI Appendix*, Table S1 in *SI Appendix*, Methods. (*H*) The majority of the mobility shift of both PER and PER-Luc is due to phosphorylation.

phase of PER2-Luc, but not the period, was dramatically altered, almost resulting in phase reversal. Similarly, *PER1* KO U2OS cells with wt PER2 had dramatic phase shift and *PER2* KO U2OS cells with wt PER1 had little altered phase when rhythms were measured using the transgenic *BMAL1-Luc* reporter (Fig. 4 *E* and *F*), showing that the phase shift was not an artifact of the PER-Luc fusion. The dramatically altered phase in PER2 rhythms in *PER1* KO cells was also confirmed by immunoblotting (Fig. 4*G*). This phase reversal is not a unique response to the use of 50% horse serum ('serum shock') as the phase-setting stimulus (zeitgeber): similar responses of *PER1* and *PER2* KOs were observed by a different zeitgeber, forskolin (*SI Appendix*, Fig. S5*B*). These data strongly suggest that the phase of all circadian genes, not just core clock genes, are phase-reversed in peripheral clock cells when *PER1* is deleted or inactivated. These data also suggest that *PER1* phase is predominant over *PER2 in* wt cells, and the resetting mechanism for *PER2* is very different from that of *PER1* as suggested above (Figs. 2 and 3). Our data are consistent with previous studies by the Schibler group showing that immediate transcriptional response to zeitgebers is very different between *Per1* and *Per2* genes (18, 41). As with mRNA levels during early hours after 2-h serum shock (18), PER1 protein increased more dramatically than PER2, but their phases were similar in wt cells (Fig. 4*H*). However, in *PER1* KO cells, PER2 profile in abundance and phosphorylation was very different from that in wt cells, further supporting that the resetting mechanism for *PER2* by zeitgebers is very different when *PER1* is present versus when it is absent.

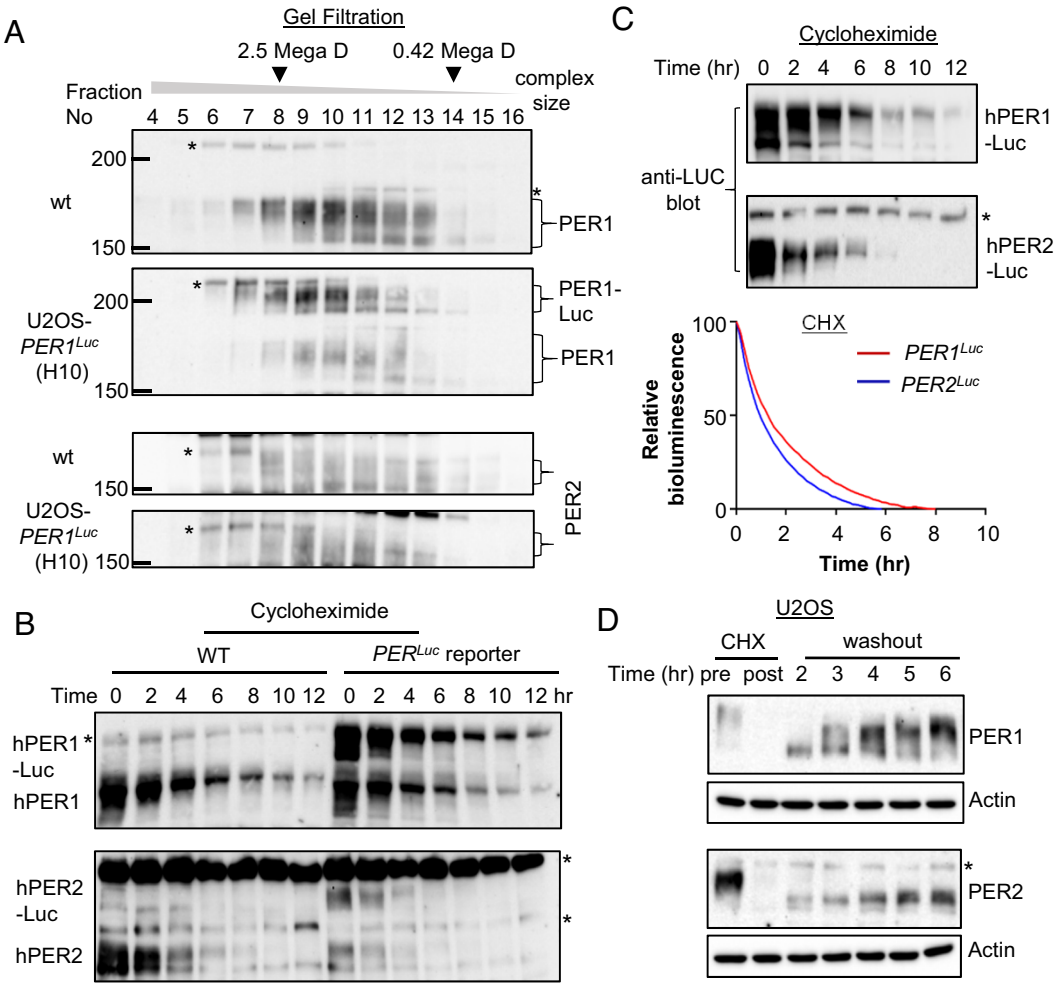

Fig. 3. PER1 and PER2 are significantly different in key parameters. (*A*) Reporter KI did not disrupt endogenous complex formation. * nonspecific band. Representative of two experiments. (*B* and *C*) PER1 was significantly more stable than PER2. Representative of three experiments. Mean of three traces are shown (n = 3, two-tailed *t* test). $P < 0.001$. (*D*) PER1 phosphorylation and accumulation were significantly faster than those of PER2 ($P < 0.001$, see *SI Appendix*, Fig. S5*A* for quantitative analysis). Existing PER was depleted by CHX treatment for 8 h (post).

***CRY* Genes Affect Circadian Rhythms through Posttranslational Regulation of PER in Addition to Transcriptional Regulation of *Per*.** CRY proteins are considered the main transcriptional inhibitors in the circadian feedback loop (42), but circadian phase (timing of feedback inhibition) is determined by cooperation between PER and CRY in the inhibitor complex (13, 43). Like the *PER* paralogs, the two *CRY* genes are not completely redundant. *CRY1* and *CRY2* KO mice show shortened and lengthened behavioral rhythms (by <1 h) compared with wt mice, respectively, suggesting that they may have a slightly antagonistic role in setting period (44, 45). To measure how they affect *PER*-reporter rhythms, *CRY1* and *CRY2* genes were singly and doubly deleted in both $PER1^{Luc}$ and $PER2^{Luc}$ KI reporter cells. Deletion of *CRY1* and *CRY2* in these cells produced period shortening and lengthening, respectively, consistent with phenotypes in mice (Fig. 5 *A*–*D*) (44, 45). However, the amount of alteration was more dramatic in U2OS cells compared with mice. Both PER1-Luc and PER2-Luc signals increased significantly in *CRY1* KO cells but slightly decreased in *CRY2* KO cells, suggesting that CRY1 is the stronger inhibitor than CRY2, consistent with recent studies (20, 21). In line with the bioluminescence data, both PER1 and PER2 protein levels were elevated in *CRY1* KO cells (Fig. 5*E*). These data elegantly explain why *CRY1* and *CRY2* KO can cause period shortening and lengthening, respectively. In *CRY1* KO cells, PER threshold levels for feedback inhibition would be reached earlier causing shortening of the feedback loop, while those would be delayed in *CRY2* KO cells resulting in period lengthening. *CRY1/2* double-KO cells did not become completely arrhythmic immediately, as opposed to immediate arrhythmicity in *CRY1/2* double-KO mice. Instead, both PER1-Luc and PER2-Luc were robustly rhythmic for one circadian cycle and then became arrhythmic (Fig. 5 *F* and *G*). The first cycle is not included because it could be zeitgeber-driven rather than an endogenous feedback loop-driven rhythm. PER1-Luc bioluminescence was higher than in wt cells, but PER2-Luc signals were slightly lower compared with wt cells. Changes in PER abundance by *CRY* KO seems to directly reflect changes in *PER* transcription in these mutant cells (Fig. 5*H*). Consistent with above data (Figs. 3 and 4), *PER1* transcription is more dramatically regulated than that of *PER2* by *CRY* KO. High and low levels of PER1 and PER2 in *CRY* double-KO cells, respectively, were confirmed by immunoblotting which also revealed an additional difference between the PER paralogs (Fig. 5 *I* and *J*). Hypophosphorylated isoforms of PER1 and PER2 were much more pronounced in *Cry* double-KO cells. Hyperphosphorylated species failed to accumulate after cycloheximide treatment (*SI Appendix*, Fig. S6*A*) suggesting that hyperphosphorylated species cannot be generated or they are very unstable without CRY. Because hyperphosphorylated PER species were readily detectable after calyculin A (CA) treatment (*SI Appendix*, Fig. S6*B*), CRY seems to protect hyperphosphorylated species from dephosphorylation or rapid degradation. Because PER, especially PER1, is more rapidly degraded in *CRY* double-KO cells

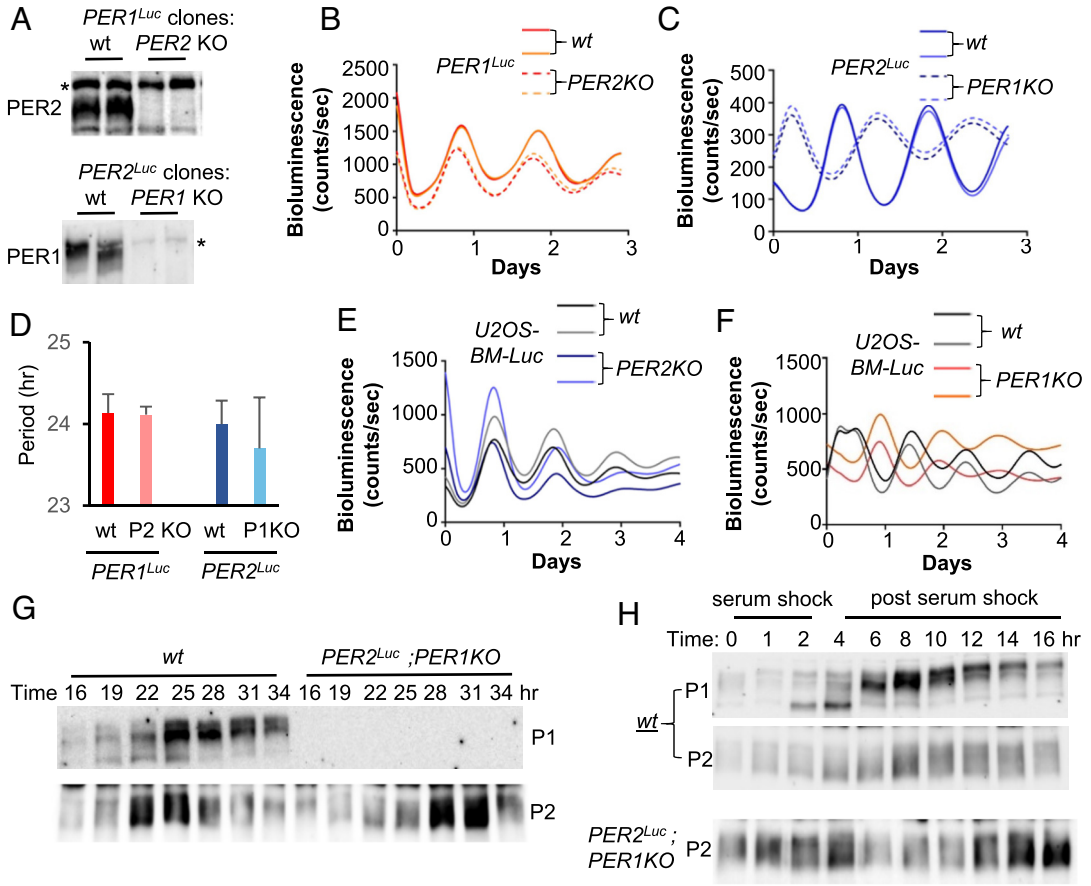

Fig. 4. *PER2* phase is reversed in the absence of the *PER1* gene in peripheral cells. (*A*) *PER* KO was screened by immunoblotting. (*B* and *C*) Bioluminescence rhythms of representative *PER2* KO in $PER1^{Luc}$ and *PER1* KO in $PER2^{Luc}$ cells are shown. Two traces are shown for each clone. n = 3 total. (*D*) Circadian period was not significantly different between *PER* KO and wt reporter cells. Mean ± SD (n = 3, two-tailed *t* test). Representative of three experiments. (*E* and *F*) *PER* KO in *BMAL1-Luc* U2OS cells showed similar results. Two traces are shown for each clone. (*G*) Antiphase oscillations of PER2 between wt and *PER1* KO cells were confirmed by immunoblotting for PER2. (*H*) Early response of PER2 to horse serum treatment (an established zeitgeber for cultured cells) was dramatically different between wt and *PER1* KO cells. Cells were given a 2-h serum shock and harvested continuously for another 14 h. Note that PER2 oscillation seems to be coupled to that of PER1 in wt cells. Representative of two experiments.

after cycloheximide (CHX) treatment (*SI Appendix*, Fig. S6*A*), these data suggest that the conversion of hypophosphorylated to hyperphosphorylated PER species is normal, but they are unstable without CRY. Similar observations were made in liver tissue between wt and *Cry* double-KO mice (19). Hyperphosphorylation of PER was restored when transgenic CRY was expressed in *CRY* double-KO cells, indicating that the phenotype is not due to the genetic defect (*SI Appendix*, Fig. S6*C*).

C Terminus of CK1δ/ε Is Critical for Rhythm Generation through Making Stable Interaction with their Substrate PER. There are seven CK1 isoforms in mammals, encoded by seven different genes (46). They are very well conserved in the catalytic domain (AA1 to ~300), but highly divergent in C-terminal noncatalytic domains (*SI Appendix*, Fig. S7). The circadian clock is completely compromised and PER hyperphosphorylation is absent in CK1δ/ε double-KO cells (47). PER2 is not even noticeably phosphorylated in the double-KO cells based on mobility shift. Although there is also evidence that CK1δ/ε are not the only kinases that phosphorylate PER (48–50), the KO data indicate that other CK1 isoforms and other kinases cannot replace CK1δ/ε as essential regulators of PER phosphorylation for the circadian clock. Because the catalytic domains are highly conserved (*SI Appendix*, Fig. S7), the C-terminal regions of CK1δ/ε are likely important for their function as circadian kinases. We began our studies of CK1δ/ε in our reporter cells by confirming their circadian functionality: deleting both genes and measuring the effect on bioluminescence rhythms. In our initial attempt to generate *CK1δ/ε* double-KO cells, we induced frame-shift mutations in exon 4 of the *CK1δ* gene, and then targeted exon 2 in *CK1ε* in the resulting *CK1δ* KO clones (*SI Appendix*, Fig. S7). However, no viable colonies were detected after single-cell sorting, indicating that double KO leads to lethality, as has been reported in MEFs (47). To circumvent this issue and test functionality of the C terminus of CK1ε at the same time, frame-shifting mutations were introduced in the nonessential C-terminal region in CK1ε (exon 8) (*SI Appendix*, Fig. S7). As expected, many viable colonies were obtained. Since our anti-CK1δ/ε antibodies were raised against the nonconserved C termini, C terminus-truncated CK1ε could not be detected on immunoblots (Fig. 6*A*). When *CK1δ* or *ε* was deleted by targeting early exons, E4 and E2, respectively, circadian rhythms were significantly lengthened by 1.5 to 2 h (Fig. 6 *B*–*D*), consistent with genetic data in mice (51). Interestingly, frame-shifting mutations in either exon 2 or exon 8 in the C terminus of CK1ε produced similarly lengthened rhythms, suggesting that the C terminus of CK1ε plays an important role in the clockwork (Fig. 6 *C* and *D*). Consistent with these data, deletion of the C terminus of CK1ε (exon 8) in a *CK1δ* KO background (thus creating double-mutant cells) produced much longer periods than *CK1δ* single-KO cells in both $PER1^{Luc}$ and $PER2^{Luc}$ cells (Fig. 6 *E*–*G* and *SI Appendix*, Fig. S8*A*), further supporting the importance of C-terminal regions in CK1δ/ε for the clockwork. One of the double mutants isolated based on period lengthening in $PER1^{Luc}$

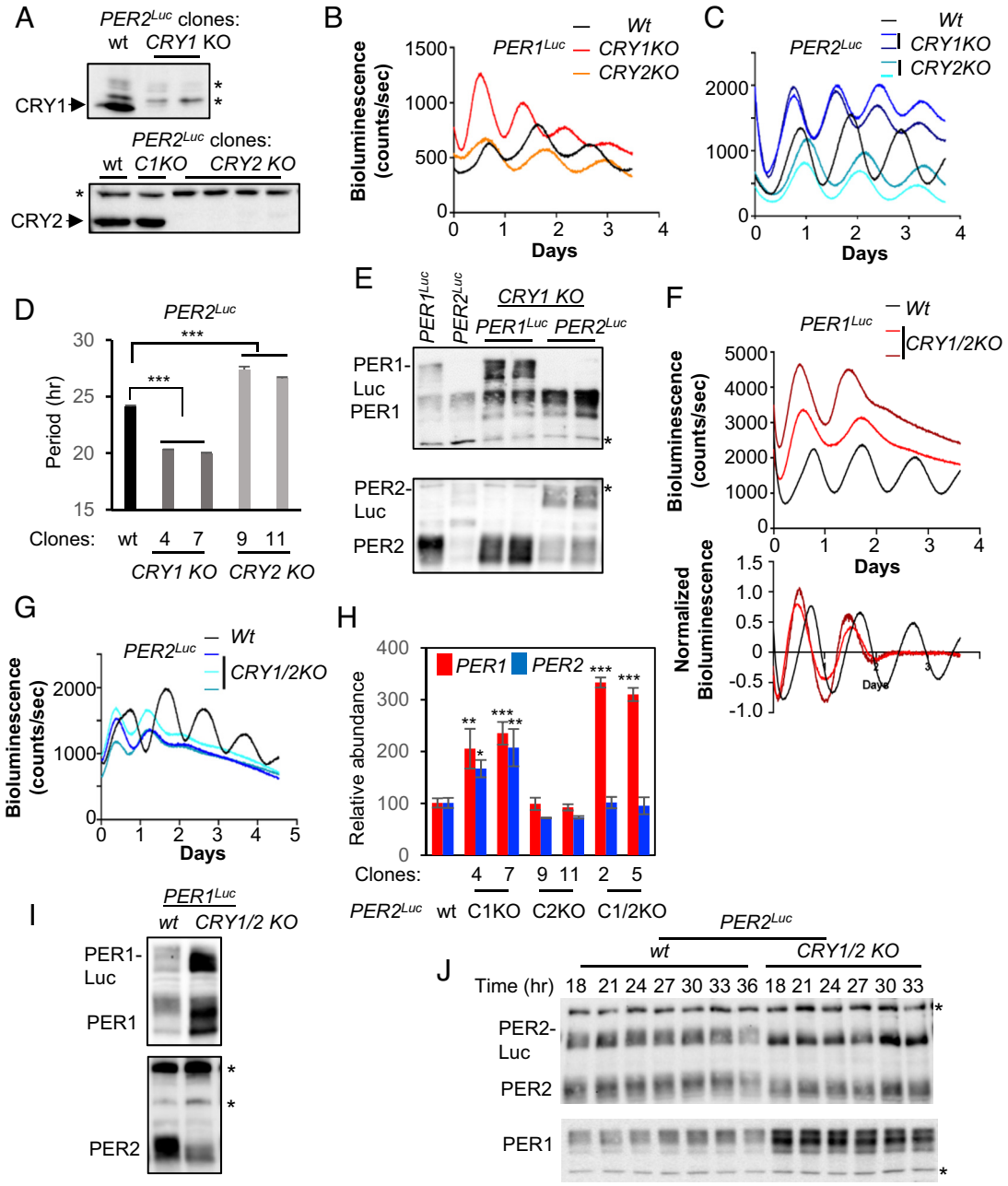

Fig. 5. Deletion of *CRY* genes in the reporter cells reveals functional difference between two CRYs. (*A*) *CRY* KOs were screened by altered bioluminescence rhythms and confirmed by immunoblotting. (*B–D*) *CRY* KO phenotypes were consistent with mouse genetics data. Each trace represents a different clone and is representative of three traces. Mean ± SD of two clones each for *CRY1* and *CRY2* KO in *Per2*^{Luc} is shown in *D* (n = 3 per clone, two-tailed *t* test). See *SI Appendix*, Table S1 in *SI Appendix*, Methods. (*E*) PER protein levels were elevated in *CRY1* KO cells. (*F* and *G*) PER1-Luc and PER2-Luc signals were higher and lower, respectively in *CRY1/2 KO*; *PER*^{Luc} reporter cells. A normalized bioluminescence graph is shown in *F* to compare apparent period between wt and *CRY1/2* double-KO cells. (*H*) Modulations of PER proteins by *CRY* KO are explainable by modulations in *PER* mRNA levels. Note that *PER1* mRNA levels were elevated in *CRY1* and *CRY1/2* KO cells but those of *PER2* mRNA were significantly elevated only in *CRY1* KO cells. Mean ± SEM of three RT-qPCR experiments (one-way ANOVA and Dunnett's post-hoc tests). See *SI Appendix*, Table S1 in *SI Appendix*, Methods for clone information. (*I*) Modulation of PER proteins in *CRY1/2* KO cells was confirmed by immunoblotting. (*J*) PER proteins are constitutively hypophosphorylated in *CRY1/2* double-KO cells. * nonspecific band.

CK1δ/ε double-mutant clones had deletion of two AAs plus a point mutation instead of a frame-shifting mutation (*PER1*^{Luc} δ/ε KO-2) (Fig. 6 *G*, *Bottom* and *SI Appendix*, Fig. S7). The mutant clone showed even longer period than a C-terminal deletion mutant clone *PER1*^{Luc} δ/ε KO-1 (Fig. 6 *F* and *G* and *SI Appendix*, Fig. S8*A*). In all of these double-mutant cells, PER could be hyperphosphorylated in a rhythmic manner albeit with a delay. There was accumulation of hyperphosphorylated PER species (Fig. 6*H*), which was probably induced by their increased stability (Fig. 6*I*). We believe the slowed hyperphosphorylation and thus increased stability are caused by attenuated interaction between PER1 and C terminus-deleted or mutated CK1ε. PER interaction with the mutant CK1ε in the *PER1*^{Luc} δ/ε KO-2 clone was significantly attenuated compared with wt CK1ε when measured using transiently expressed proteins (Fig. 6*J*). Consistent with the above findings, when the *PER2*^{Luc} δ/ε KO cells were rescued with wt *CK1ε* transgene, the period of the double-mutant clone was almost normalized to ~25 h, while rescue with the mutant (ΔRE) *CK1ε* did not significantly alter the period of the double-mutant cells (*SI Appendix*, Fig. S8*B*). Overall, these data suggest that C-terminal regions of CK1δ/ε play an important role

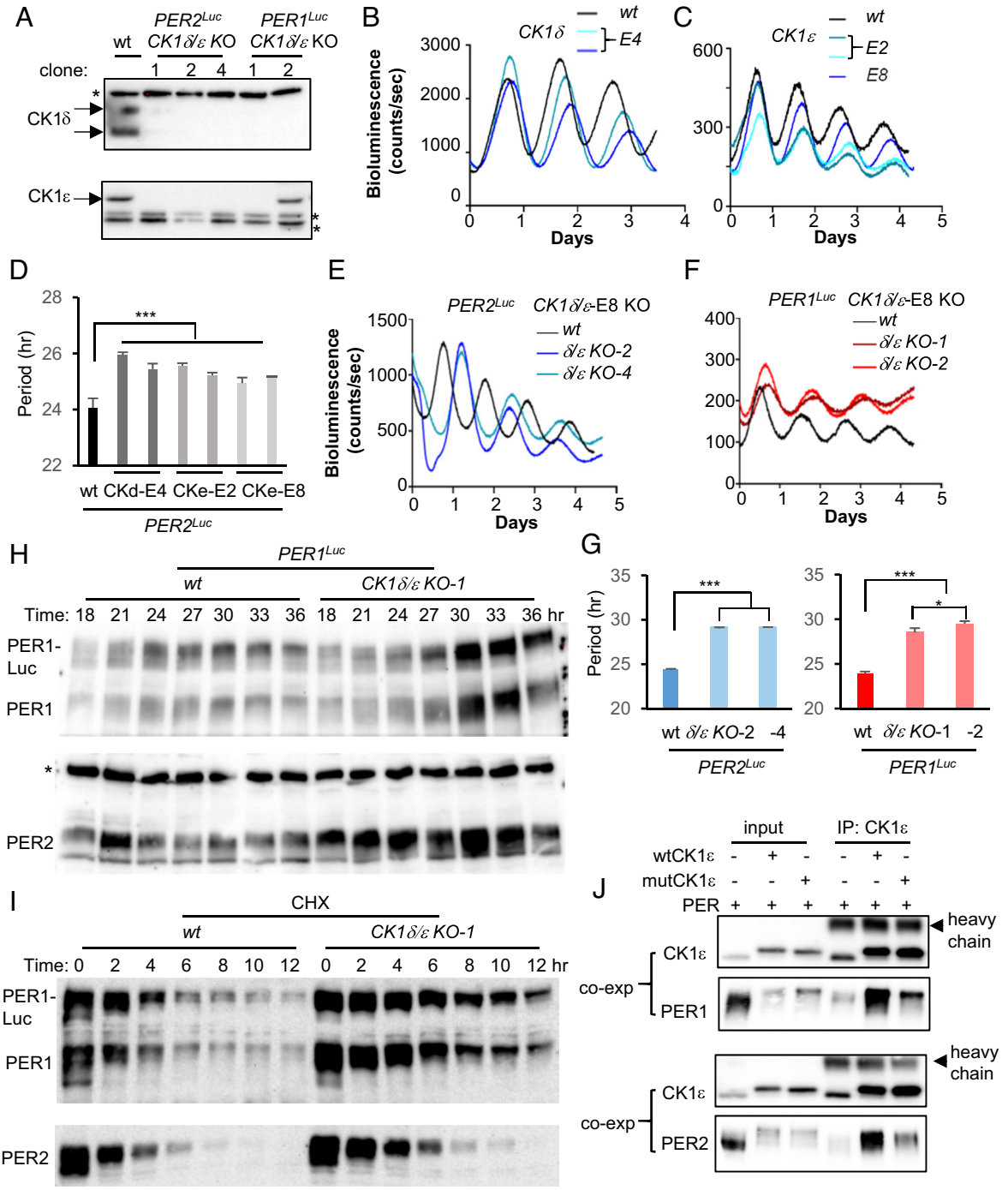

Fig. 6. C-termini of CK1δ/ε play important roles in rhythm generation. (*A*) Deletion of *CK1δ/ε* was screened by altered bioluminescence rhythms and confirmed by immunoblotting. * nonspecific band. Note that CK1ε is detected in double KO #2 in *PER1*^{Luc} reporter cell due to an in-frame mutation in one allele (*Per1*^{Luc} *δ/ε* KO-2) (*SI Appendix*, Fig. S7). (*B* and *D*) Single KOs of *CK1δ* and *CK1ε* and C terminus deletion of CK1ε all lead to lengthened rhythms. Two representative clones for each KO are shown in *D*. Mean ± SD (n = 3 per clone, two-tailed *t* test). (*E–G*) *CK1δ/ε* double-mutant clones showed dramatically lengthened rhythms. Note that *δ/ε* KO-2 in *F* represents the double-mutant clone with the in-frame mutation in C terminus instead of a complete KO via a frame-shifting mutation. Mean ± SD (n = 3 per clone, two-tailed *t* test). (*H*) Hyperphosphorylated PER species were pronounced in CK1 double-mutant cells. *δ/ε* KO-1 clone in *PER1*^{Luc} reporter cell is shown. * nonspecific band. (*I*) PER, especially PER1 was stabilized in double-mutant clones. *δ/ε* KO-1 clone in *PER1*^{Luc} reporter cell is shown. (*J*) PER interaction with a mutant CK1ε with two AA deletion (CK1εΔRE) in C terminus was significantly attenuated. PER was coexpressed with wt CK1ε or mut CK1ε and subjected to coimmunoprecipitation. Note that small amounts of transgenic PER were copurified with endogenous CK1ε by the anti-CK1ε antibody. Transgenic CK1ε is larger than the endogenous counterpart by 18 AAs.

in promoting hyperphosphorylation in PER for timely degradation through making stable interactions between enzyme and substrate.

The Circadian Phosphotimer Requires Stable Interaction between CK1δ/ε and PER. Two main events regulated by the PER phosphotimer are nuclear entry and degradation of the PER-containing complex; these events are separated by ~12 h and define distinct circadian phases (19, 38, 47). Because PER phosphorylation by CK1δ/ε is responsible for these events directly, the timing of PER phosphorylation must occur over the same extended period, ~12 h. CK1δ and ε bind the substrate PER stably through a dedicated ~220 AA domain called CKBD in PER (22, 52), which is different from a typical transient kinase–substrate relationship. Although many previous studies suggested that this domain (which, as discussed

earlier, contains the FASPS mutation S662G) plays an important role in setting period, how CKBD contributes to the phosphotimer has been unsolved. While generating AA indels around S662 in CKBD by CRISPR to study the significance of the domain, a mutant clone missing 2/3 of CKBD was isolated (Fig. 7*A* and *SI Appendix*, Fig. S8*C*). This clone exhibited a significantly lengthened rhythm, ~27.5 h (Fig. 7 *A* and *B*). The mutant PER2 levels were elevated compared with wt PER2. When *Per1* was deleted in this clone, rhythms were completely eliminated, and protein levels were further elevated, demonstrating that the mutant PER2 is not functional, and the mutation is semidominant over *Per1* (Fig. 7*A*). The mutant PER2 was constitutively hyperphosphorylated, which was not dependent on PER1 (Fig. 7 *C* and *D*). As expected, its interaction with CK1δ/ε was dramatically attenuated (*SI Appendix*, Fig. S8*D*). Although these data indicate that PER hyperphosphorylation is not dependent on stable interaction with CK1δ/ε, when the mutant cell was treated with a specific CK1δ/ε inhibitor, PF670462, PER hyperphosphorylation was inhibited in both wt and mutant PER2, demonstrating that hyperphosphorylation of the mutant PER2 does depend on CK1δ/ε (Fig. 7*E* and *SI Appendix*, Fig. S8*E*). Furthermore, hyperphosphorylation of the mutant PER2 was more sensitive to the inhibitor; maximum inhibition was achieved at a much lower dose of the inhibitor compared with wt PER2 (Fig. 7*E* and *SI Appendix*, Fig. S8*E*). These data suggest that hyperphosphorylation of PER by CK1δ/ε does not require stable interaction, but a functional phosphotimer requires CKBD because it can allow slow and progressive phosphorylation. In the absence of the stable interaction, PER phosphorylation by the kinases would be done in a transient manner like typical kinase reactions. The mutant PER2 was predominantly nuclear as expected from their phosphorylation status and significantly more stable than wt PER2 (Fig. 7 *F* and *G* and *SI Appendix*, Fig. S9). When the mutant PER2 was treated with CA, extra hyperphosphorylated species were not detected, suggesting that this mutant PER2 is defective in this extra phosphorylation, which is normally not detected in a steady state because these extra hyperphosphorylated species are rapidly turned over by β-TRCP-regulated proteasomal degradation (Fig. 7*H*) (38). Faster phosphorylation kinetics for the mutant PER2 was confirmed with de novo PER2 after existing PERs was depleted (Fig. 7*I*). The lack of extra hyperphosphorylation was reproduced with transiently expressed CK1δ and mutant PER2 (Fig. 7*J*).

Discussion

A critical bottleneck in studying complex biological systems like the circadian clock is the lack of an efficient in vivo-like platform where endogenous genes can be easily manipulated to test diverse hypotheses in a time- and cost-effective manner. Historically, manipulation of endogenous clock genes in cell culture models required first developing mutant mouse models from which cells such as MEFs were then harvested (38, 53, 54). However, recent developments in CRISPR genome editing have created new opportunities for generating cell culture models without first generating mutant mice. Several studies including ours demonstrated that clock genes can be knocked out efficiently in culture using CRISPR (55–59). One key limitation in cell models today is the lack of precise endogenous phase and period reporters working like clock hands other than the *mPer2-Luc* reporter in MEFs. Fluorescence reporters have been developed (60), but they are far less accurate than bioluminescence reporters and require heavy deconvolution of data, especially when signal is barely above background. When we put mRuby3 before Luc to produce the PER-mRuby3 fusion protein, fluorescence signal was significantly lower than nonfusion mRuby3 and barely above background when measured by FACS and microscopy. This is probably due to decreased stability of mRuby3 when it is attached to the unstable PER. We were able to observe robust rhythms for more than 10 d from our bioluminescence reporter cells compared with 2 to 3 d reported using fluorescence reporters (60).

Fusion of a fairly large protein, Luc, to PER did not seem to affect phosphorylation and stability of PER, which suggests a dominant regulation of PER at the posttranslational level and can explain a wt-like circadian phenotype in the $mPer2^{Luc}$ KI mouse. Although PER1 and PER2 are independently rhythmic in abundance and phosphorylation and redundant in generation of circadian rhythms, their kinetics such as stability and speed of phosphorylation differ significantly. In addition, *PER1* and *PER2* oscillations are also likely differentially affected at the level of negative feedback transcriptional kinetics as their mRNA levels are differently regulated in the absence of the feedback inhibitors, CRY KO. Because PER protein phase and thus the phase in the feedback loop would be determined by these properties, it would be expected that the phase of ccgs would be different between *Per1* and *Per2* KO cells. Indeed, the phase of *BMAL1-Luc* was reversed in *PER1* KO, but not in *PER2* KO cells, suggesting that *PER1* phase is dominant over that of *PER2* in wt cells, probably due to higher abundance and leading phosphorylation kinetics. However, the circadian phase of the master clock in the SCN is not altered in *PER1* KO mice. Both *PER1* and *PER2* KO mice show similar phases in behavioral rhythms in constant darkness after LD entrainment (17). We believe the difference between peripheral and master clocks is due to different entrainment mechanisms. In the master clock, both *Per* genes are rapidly induced by photic signals resulting in acute phase shifting (39). However, in peripheral cells, *Per2* rhythm is not rapidly reset by zeitgebers because its transcription is not acutely induced while *Per1* rhythm is acutely reset by these signals through rapid induction of mRNA as in SCN by photic signals (18). This has a significant implication in humans with a defective *PER1* gene because their peripheral clocks could be dissociated from the SCN clock.

Because PER-Luc oscillates with a circadian period in *CRY1/2* KO cells at least for one complete cycle (57, 61), PER alone seems to act as a feedback inhibitor, but the clock cannot be sustained without CRY. PER can directly interact with CLOCK:BMAL1 and repress the activity of the complex in in vitro reporter assays supporting the inhibitory role (13, 42). In *β-Trcp* mutant cells, the clock cannot be sustained because hyperphosphorylated PER species are too stable in the nucleus (38). Similarly, it may be that the clock cannot be sustained in *CRY1/2* KO cells because hyperphosphorylated PER species are too unstable, and CRY is necessary to extend nuclear presence of PER and PER-containing inhibitory complexes.

Our data suggest that the progressive and controlled phosphorylation of PER is mediated by stable interaction between the kinase and substrate resulting in slowing down kinase movement (processivity) on PER for serial phosphorylation. The phosphotimer can be also modulated by mutations in CK1δ/ε. CK1s are considered anion- or phosphate-binding kinases because basic AAs in the anion-binding pockets interact with anions or phosphate groups on substrates (62, 63). CK1s depend on negative charges or prior phosphorylation on a substrate for processive phosphorylation as in a typical consensus motif pSxxS (25, 62, 63), which appears throughout the entire PER1 and PER2 protein, not just the FASPS domain, yet current working models of the clockwork focus on only two motifs, FASPS and a degron motif (25, 64). CK1s have several substrate-facing, anion-binding pockets; thus the more PER is phosphorylated

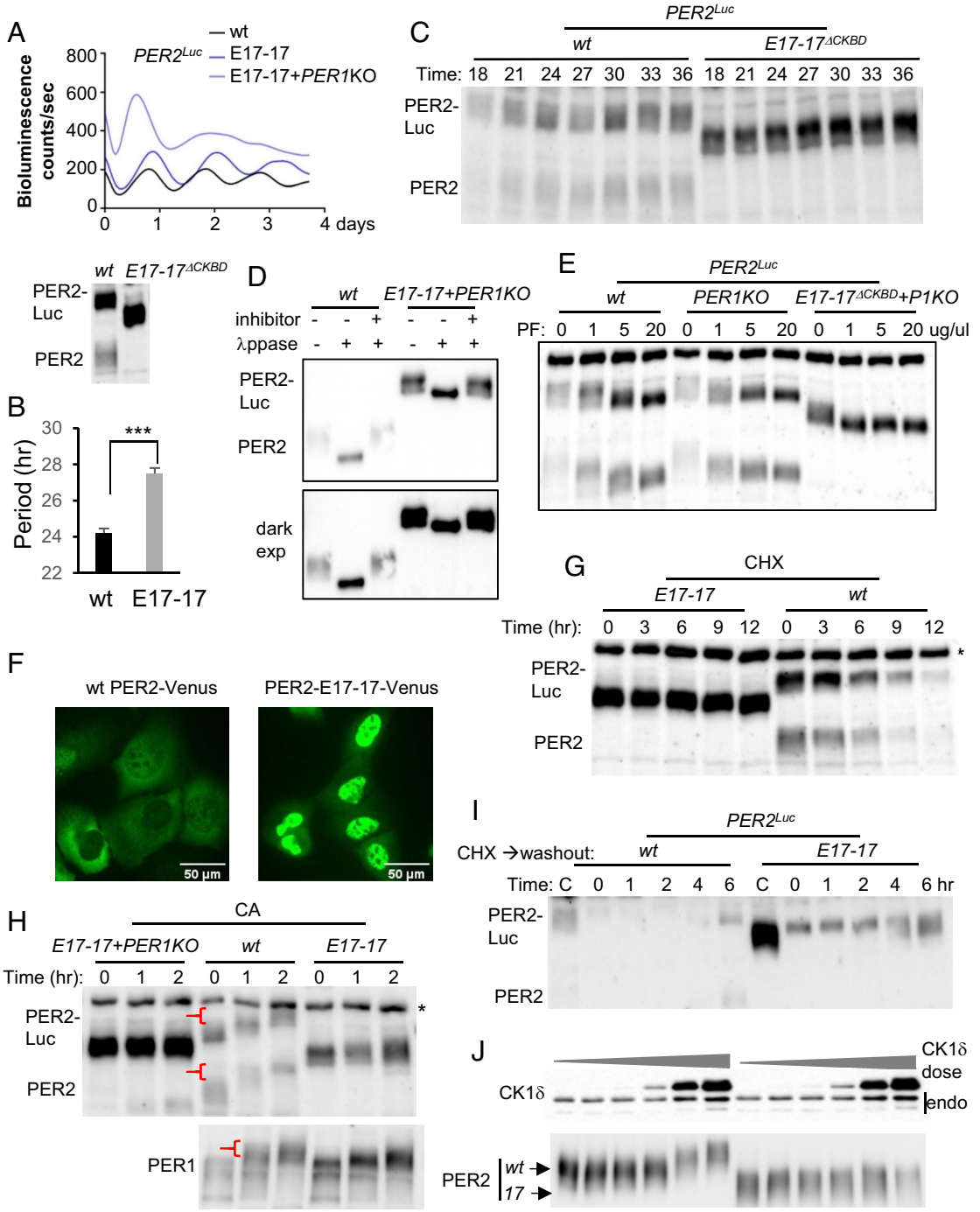

Fig. 7. CKBD allows for slow progressive phosphorylation kinetics essential for the phosphotimer. (*A* and *B*) A *PER2* mutant clone lacking the CKBD showed lengthened rhythms in a *PER1* wt background but arrhythmicity in *PER1* KO cells. Note that PER2-Luc signals were elevated in *PER1* wt and further elevated in the *PER1* KO background. A similar number of cells was used. A smaller size mutant protein was confirmed by sequencing of cDNA (*SI Appendix*, Fig. S8*C*) and immunoblotting (*Bottom* panel in *A*). (*C*) The mutant PER2 seemed to be constitutively hyperphosphorylated based on mobility shift on the immunoblot. (*D*) Hyperphosphorylation was confirmed by phosphatase treatment. Two exposures are shown. Representative of two experiments. (*E*) Phosphorylation of the mutant PER2 is mediated by CK1δ/ε. Lower doses were used in *SI Appendix*, Fig. S8*E*. (*F*) The mutant PER2 was constitutively nuclear. Wt PER2 was detectable in both cytoplasm and nucleus. When wt PER2 was expressed in high amounts, they were predominantly cytoplasmic (*SI Appendix*, Fig. S9) (37). (*G*) The mutant PER2 was significantly more stable than wt PER2. (*H*) The mutant PER2 was not additionally phosphorylated by CA treatment. PER1/2 in wt cells are extra hyperphosphorylated by CA treatment (indicated by red half left parenthesis). See extra hyperphosphorylation in *SI Appendix*, Fig. S6*B*). (*I*) Phosphorylation of de novo mutant PER2 was significantly advanced compared with its wt counterpart. Time '0 h' represents 8 h after CHX treatment right before washout. Note that a significant amount of the mutant PER2 still existed after CHX treatment. (*J*) The mutant PER2 is less phosphorylated in vitro by CK1δ compared with wt PER2. Increasing amounts of CK1δ were coexpressed with a fixed amount of PER2.

in CKBD, the more robustly PER will hold CK1, resulting in slower processivity. In vivo, CK1δ/ε are predominantly copurified only with hyperphosphorylated PER species (19), supporting the model. Further, charge inversion mutations such as *tau* (R178C) and K224D in one of the anion-binding pockets of CK1 accelerate the phosphotimer and the clock (64, 65). Consistent with this model, deletion of the whole CKBD resulted in typical rapid kinase reactions, leading to constitutive or nonprogressive hyperphosphorylation. This level of phosphorylation was enough for nuclear entry, but not for degradation

as shown in Fig. 7. The PER phosphotimer seems to have two distinctive phases, one for nuclear entry and the other for degradation, matching with onset and offset sleep phases. CKBD is required for the second phase of the phosphotimer. It is not clear whether CKBD itself contains a critical phosphodegron or whether stable CK1 binding to PER is required for phosphorylation in a degron somewhere else in PER. The C terminus of CK1ε, probably the C terminus of CK1δ too, is not required for progressive phosphorylation itself as the deletion of the C terminus produced intact progressive phosphorylation albeit at a slower rate. Because the deletion of the C terminus produced lengthened rhythms, we believe it modulates the speed of progressive phosphorylation.

The phosphotimer is at the heart of the circadian clock; it is the basis for how a cell can measure time precisely over timeframes much longer than typical cellular processes. Our studies revealed many critical properties of this timer using diverse clock mutants. In addition, our human reporter cell model could provide direct insights into pathogenicity of many period- and phase-altering mutations in CK1 and PER and serve as an efficient platform to test diverse hypotheses developed via human genetics and biochemical studies.

Materials and Methods

Cell Lines. The U2OS cell line was purchased from American Type Culture Collection (ATCC) (#HTB-96).

U2OS-Bmal1-Luc wt and *PER2* KO (E5-2) lines were described previously (57). U2OS-Bmal1-Luc; *PER1* KO clones were selected from the previous study (57), and #E6-2-4 was used for this study.

mPer2^{Luc} KI reporter MEFs were described previously (26).

HEK293a (ThermoFisher #70507) was used in Fig. 6*J*.

All cells were maintained at 37 °C, 5% CO_2 in DMEM, supplemented with 10% FBS.

Generation of *Per* KI Cell Lines. For all CRISPR-induced mutations, sgRNAs were selected via CHOPCHOP (https://chopchop.cbu.uib.no), cloned into pAdTrack-Cas9-DEST, and tested for efficiency by T7E1 assay as described previously [Jin et al. (57)].

wt U2OS cells were transfected with all-in-one pAdTrack-Cas9-DEST plasmids (sgRNA sequence described in *SI Appendix*, Table S1 and T7E1 primers described in *SI Appendix*, Table S2) and linear repair templates (*SI Appendix*, Figs. S10 and S11) using jetOPTIMUS according to the manufacturer's protocol (jetOPTIMUS transfection reagent, Polyplus). The linear templates were prepared from Per-Luc-T2A-Ruby_pUC19 plasmid (*SI Appendix*, Fig. S12) by PCR amplification. Cloning primers for the plasmids are described in *SI Appendix*, Table S3 and Fig. S12. Assembly of these amplicons were done using New England Biolabs (NEB) HiFi DNA Assembly Master Mix according to the manufacturer's protocol.

The transfected cells were maintained and expanded for 10 d before they were subjected to trypsinization and FACS sorting using BD FACSAria Special Order Research Product (SORP) equipped with an Automated Cell Deposition Unit for mRuby3-positive single-cell sorting into 96-well plates as well as bulk sorting. The single cells were expanded for 2 wk and split into one well in a regular 24-well plate and one well in a black-wall 24-well plate (PerkinElmer #1450-605, Arkon, OH, USA). The bulk sorted cells were also added into the black-wall plate before it was set up into Lumicycle 96. Several clones with robust circadian bioluminescence rhythms were selected for each *Per* gene and subjected to junction PCR, immunoblotting with anti-PER1 (GP62), anti-PER2 (hP2-GP49) and anti-Luc antibodies, and Sanger sequencing. For Luc immunoblotting, novel polyclonal anti-Luc antibodies were generated by Cocalico Biologicals, Inc (449 Stevens Rd, Reamstown, PA) in guinea pigs using Luc AA 300 to 550 peptide. The antisera were validated against transfected Luc and Luc KI cells. GP77 was used in this study. To verify a single insertion of the dual reporter, frameshift mutations were introduced in early exons in these clones using all-in-one CRISPR adenovirus as described previously (57) (*SI Appendix*, Fig. S3). Disappearance of mRuby3 signal was confirmed by fluorescence microscopy and by FACS and bioluminescence in the Lumicycle 96. Final positive clones are summarized in *SI Appendix*, Table S1.

Mutations of Clock Genes in *PER1*^{Luc} and *PER2*^{Luc} Reporter Cells. Het KI clones, H10 for *PER1*^{Luc} and LH1 for *PER2*^{Luc}, were used to generate mutations in other clock genes. The mRuby3-expressing reporter cells were transfected with all-in-one pAdTrack-Cas9-DEST plasmids expressing GFP. In *SI Appendix*, Fig. S3, the reporter cells were infected with all-in-one CRISPR adenovirus to induce indels in the majority of the cells with near 100% efficiency as described previously. For clonal isolation of clock mutant cells, GFP-positive cells were sorted by FACS into 96-well plates, and these clones were further selected based on alterations in period and/or phase in bioluminescence rhythms. The sgRNA sequence and final clones are summarized in *SI Appendix*, Table S1. In each project, the majority of putative mutant clones showed a similar degree of period lengthening or shortening in bioluminescence screening. Some of these mutant clones were fully characterized by immunoblotting and sequencing.

***PER* Mutant Clones in *PER*^{Luc} Reporter Cell Lines.** All-in-one adenovirus expressing CAS9 and *PER1*-E6 sgRNA used to generate indels in the *PER1* gene were described previously (57). For Fig. 4*C*, single *PER1* KO clones were isolated by FACS followed by immunoblotting and a clone #*PER1*-E6-11 was used. To generate all-in-one adenovirus targeting *PER2* exon 6 or exon 17, the following sgRNA sequence was cloned into the pAdTrack-Cas9-Dest, and adenoviruses were packaged as described previously (57).

Gene	Target	sgRNA sequence (Protospacer Adjacent Motif)	Selected clones
PER2	Exon 6	ATCTCTTTTACAGT-GAAATA(TGG)	*PER2*-E6-7, 55
PER2	Exon 17	GCCGGGCAAGGCAGA-GAGTG(TGG)	*PER2*-E17-17

For Fig. 4*B*, single *PER2* KO clones were isolated using *Adv-PER2-E6* as described above. Clone #*PER2*-E6-55 was used. To generate in-frame indels in *PER2* exon 17, the *Adv-PER2-E17* was infected into the *PER2*^{Luc} reporter cells, and mRuby3-positive cells were sorted into 96-well plates by FACS. These cells are either wt or in-frame mutant cells because mRuby3 will be eliminated by out-of-frame mutations. One of the mutants was E17-17 which is missing 2/3 of CKBD. To delete *PER1* in this clone, *Adv-PER1-E6* was infected into the cells, and *PER1* KO was confirmed by immunoblotting.

Genotyping. For *PER* KI clones, KI and non-KI alleles from each clone were PCR-amplified using the primers described in *SI Appendix*, Table S4 and Fig. S13, and the amplicons were sequenced using primers described in *SI Appendix*, Table S5.

For mutant clones with indels, amplicons of the target regions were prepared using the surveyor primers (*SI Appendix*, Table S2) and sequenced. In the majority of the clones, two different Sanger sequencing traces were mixed due to different indels in two alleles. These results were deconvoluted by a computer algorithm called DECORD v3 (https://decodr.org/) into two separate traces. Accuracy of the deconvolution was confirmed by TA cloning of several amplicons from several mutant clones. Frameshift mutations in one or both alleles were also confirmed by immunoblotting.

See *SI Appendix, Extended Materials and Methods*.

Data, Materials, and Software Availability. All study data are included in the article and/or *SI Appendix*.

ACKNOWLEDGMENTS. We thank Dennis Chang for assistance with manuscript revisions and Robert Tomko for gel filtration chromatography. We thank Jonathan M. Philpott and Carrie L. Partch for critical reading of the manuscript and providing feedback. This work was supported by NIH R01 GM131283 awarded to C.L. and by Korea Institute for Advancement of Technology (P0002007, Human Resource Development (HRD) Program for Industrial Innovation) grant to H.S.

Author affiliations: [a]Department of Biomedical Sciences, Program in Neuroscience, College of Medicine, Florida State University, Tallahassee, FL 32306; and [b]Department of Chemical Engineering and Biotechnology, Tech University of Korea, 15073 237 Gyeonggi-do, Republic of Korea

1. S. M. Reppert, D. R. Weaver, Coordination of circadian timing in mammals. *Nature* **418**, 935–941 (2002).
2. U. Schibler, The daily rhythms of genes, cells and organs. Biological clocks and circadian timing in cells. *EMBO Rep.* **6 Spec No**, S9–S13 (2005).
3. D. Bell-Pedersen *et al.*, Circadian rhythms from multiple oscillators: Lessons from diverse organisms. *Nat. Rev. Genet.* **6**, 544–556 (2005).
4. J. A. Mohawk, C. B. Green, J. S. Takahashi, Central and peripheral circadian clocks in mammals. *Annu. Rev. Neurosci.* **35**, 445–462 (2012).
5. S. L. Harmer, S. Panda, S. A. Kay, Molecular bases of circadian rhythms. *Annu. Rev. Cell Dev. Biol.* **17**, 215–253 (2001).
6. C. B. Green, J. S. Takahashi, J. Bass, The meter of metabolism. *Cell* **134**, 728–742 (2008).
7. C. L. Drake, T. Roehrs, G. Richardson, J. K. Walsh, T. Roth, Shift work sleep disorder: Prevalence and consequences beyond that of symptomatic day workers. *Sleep* **27**, 1453–1462 (2004).
8. J. Bass, J. S. Takahashi, Circadian integration of metabolism and energetics. *Science* **330**, 1349–1354 (2010).
9. L. Zhu, P. C. Zee, Circadian rhythm sleep disorders. *Neurol. Clin.* **30**, 1167–1191 (2012).
10. E. S. Musiek *et al.*, Circadian clock proteins regulate neuronal redox homeostasis and neurodegeneration. *J. Clin. Invest.* **123**, 5389–5400 (2013).
11. A. Patke, M. W. Young, S. Axelrod, Molecular mechanisms and physiological importance of circadian rhythms. *Nat. Rev. Mol. Cell Biol.* **21**, 67–84 (2020).
12. G. D. Potter *et al.*, Circadian rhythm and sleep disruption: Causes, metabolic consequences, and countermeasures. *Endocr. Rev.* **37**, 584–608 (2016).
13. R. Chen *et al.*, Rhythmic PER abundance defines a critical nodal point for negative feedback within the circadian clock mechanism. *Mol. Cell* **36**, 417–430 (2009).
14. K. L. Toh *et al.*, An hPer2 phosphorylation site mutation in familial advanced sleep phase syndrome. *Science* **291**, 1040–1043 (2001).
15. P. L. Lowrey *et al.*, Positional syntenic cloning and functional characterization of the mammalian circadian mutation tau. *Science* **288**, 483–492 (2000).
16. L. P. Shearman, X. Jin, C. Lee, S. M. Reppert, D. R. Weaver, Targeted disruption of the mPer3 gene: Subtle effects on circadian clock function. *Mol. Cell Biol.* **20**, 6269–6275 (2000).
17. J. S. Pendergast, R. C. Friday, S. Yamazaki, Photic entrainment of period mutant mice is predicted from their phase response curves. *J. Neurosci.* **30**, 12179–12184 (2010).
18. A. Balsalobre, L. Marcacci, U. Schibler, Multiple signaling pathways elicit circadian gene expression in cultured Rat-1 fibroblasts. *Curr. Biol.* **10**, 1291–1294 (2000).
19. C. Lee, J. P. Etchegaray, F. R. Cagampang, A. S. Loudon, S. M. Reppert, Posttranslational mechanisms regulate the mammalian circadian clock. *Cell* **107**, 855–867 (2001).
20. C. Rosensweig *et al.*, An evolutionary hotspot defines functional differences between CRYPTOCHROMES. *Nat. Commun.* **9**, 1138 (2018).
21. J. L. Fribourgh *et al.*, Dynamics at the serine loop underlie differential affinity of cryptochromes for CLOCK:BMAL1 to control circadian timing. *Elife* **9**, e55275 (2020).
22. C. Lee, D. R. Weaver, S. M. Reppert, Direct association between mouse PERIOD and CKIepsilon is critical for a functioning circadian clock. *Mol. Cell Biol.* **24**, 584–594 (2004).
23. E. Vielhaber, E. Eide, A. Rivers, Z. H. Gao, D. M. Virshup, Nuclear entry of the circadian regulator mPER1 is controlled by mammalian casein kinase I epsilon. *Mol. Cell Biol.* **20**, 4888–4899 (2000).
24. R. Narasimamurthy *et al.*, CK1delta/epsilon protein kinase primes the PER2 circadian phosphoswitch. *Proc. Natl. Acad. Sci. U.S.A.* **115**, 5986–5991 (2018).
25. J. M. Philpott *et al.*, Casein kinase 1 dynamics underlie substrate selectivity and the PER2 circadian phosphoswitch. *Elife* **9**, e52343 (2020).
26. S. H. Yoo *et al.*, PERIOD2::LUCIFERASE real-time reporting of circadian dynamics reveals persistent circadian oscillations in mouse peripheral tissues. *Proc. Natl. Acad. Sci. U.S.A.* **101**, 5339–5346 (2004).
27. A. C. Liu, W. G. Lewis, S. A. Kay, Mammalian circadian signaling networks and therapeutic targets. *Nat. Chem. Biol.* **3**, 630–639 (2007).
28. B. Maier *et al.*, A large-scale functional RNAi screen reveals a role for CK2 in the mammalian circadian clock. *Genes. Dev.* **23**, 708–718 (2009).
29. S. Yamazaki *et al.*, Resetting central and peripheral circadian oscillators in transgenic rats. *Science* **288**, 682–685 (2000).
30. F. Uddin, C. M. Rudin, T. Sen, CRISPR gene therapy: Applications, limitations, and implications for the future. *Front. Oncol.* **10**, 1387 (2020).
31. X. H. Zhang, L. Y. Tee, X. G. Wang, Q. S. Huang, S. H. Yang, Off-target effects in CRISPR/Cas9-mediated genome engineering. *Mol. Ther. Nucleic Acids* **4**, e264 (2015).
32. B. Koch *et al.*, Generation and validation of homozygous fluorescent knock-in cells using CRISPR-Cas9 genome editing. *Nat. Protoc.* **13**, 1465–1487 (2018).
33. B. P. Kleinstiver *et al.*, High-fidelity CRISPR-Cas9 nucleases with no detectable genome-wide off-target effects. *Nature* **529**, 490–495 (2016).
34. I. M. Slaymaker *et al.*, Rationally engineered Cas9 nucleases with improved specificity. *Science* **351**, 84–88 (2016).
35. F. A. Ran *et al.*, Genome engineering using the CRISPR-Cas9 system. *Nat. Protoc.* **8**, 2281–2308 (2013).
36. N. J. Smyllie *et al.*, Visualizing and quantifying intracellular behavior and abundance of the core circadian clock protein PERIOD2. *Curr. Biol.* **26**, 1880–1886 (2016).
37. S. Beesley *et al.*, Wake-sleep cycles are severely disrupted by diseases affecting cytoplasmic homeostasis. *Proc. Natl. Acad. Sci. U.S.A.* **117**, 28402–28411 (2020).
38. M. D'Alessandro *et al.*, Stability of wake-sleep cycles requires robust degradation of the PERIOD protein. *Curr. Biol.* **27**, 3454–3467.e8 (2017).
39. S. M. Reppert, D. R. Weaver, Molecular analysis of mammalian circadian rhythms. *Annu. Rev. Physiol.* **63**, 647–676 (2001).
40. Y. Shigeyoshi *et al.*, Light-induced resetting of a mammalian circadian clock is associated with rapid induction of the mPer1 transcript. *Cell* **91**, 1043–1053 (1997).
41. A. Balsalobre, F. Damiola, U. Schibler, A serum shock induces circadian gene expression in mammalian tissue culture cells. *Cell* **93**, 929–937 (1998).
42. K. Kume *et al.*, mCRY1 and mCRY2 are essential components of the negative limb of the circadian clock feedback loop. *Cell* **98**, 193–205 (1999).
43. M. Ukai-Tadenuma *et al.*, Delay in feedback repression by cryptochrome 1 is required for circadian clock function. *Cell* **144**, 268–281 (2011).
44. G. T. van der Horst *et al.*, Mammalian Cry1 and Cry2 are essential for maintenance of circadian rhythms. *Nature* **398**, 627–630 (1999).
45. M. H. Vitaterna *et al.*, Differential regulation of mammalian period genes and circadian rhythmicity by cryptochromes 1 and 2. *Proc. Natl. Acad. Sci. U.S.A.* **96**, 12114–12119 (1999).
46. U. Knippschild *et al.*, The CK1 family: Contribution to cellular stress response and its role in carcinogenesis. *Front. Oncol.* **4**, 96 (2014).
47. H. M. Lee *et al.*, The period of the circadian oscillator is primarily determined by the balance between casein kinase 1 and protein phosphatase 1. *Proc. Natl. Acad. Sci. U.S.A.* **108**, 16451–16456 (2011).
48. T. Hirota *et al.*, High-throughput chemical screen identifies a novel potent modulator of cellular circadian rhythms and reveals CKIalpha as a clock regulatory kinase. *PLoS Biol.* **8**, e1000559 (2010).
49. E. M. Smith, J. M. Lin, R. A. Meissner, R. Allada, Dominant-negative CK2alpha induces potent effects on circadian rhythmicity. *PLoS Genet.* **4**, e12 (2008).
50. J. C. Chiu, H. W. Ko, I. Edery, NEMO/NLK phosphorylates PERIOD to initiate a time-delay phosphorylation circuit that sets circadian clock speed. *Cell* **145**, 357–370 (2011).
51. J. P. Etchegaray *et al.*, Casein kinase 1 delta regulates the pace of the mammalian circadian clock. *Mol. Cell Biol.* **29**, 3853–3866 (2009).
52. E. J. Eide *et al.*, Control of mammalian circadian rhythm by CKIepsilon-regulated proteasome-mediated PER2 degradation. *Mol. Cell Biol.* **25**, 2795–2807 (2005).
53. H. Xu *et al.*, Cryptochrome 1 regulates the circadian clock through dynamic interactions with the BMAL1 C terminus. *Nat. Struct. Mol. Biol.* **22**, 476–484 (2015).
54. N. Park *et al.*, A novel Bmal1 mutant mouse reveals essential roles of the C-terminal domain on circadian rhythms. *PLoS One* **10**, e0138661 (2015).
55. S. Korge, A. Grudziecki, A. Kramer, Highly efficient genome editing via CRISPR/Cas9 to create clock gene knockout cells. *J. Biol. Rhythms* **30**, 389–395 (2015).
56. C. Lu *et al.*, Role of circadian gene clock during differentiation of mouse pluripotent stem cells. *Protein Cell* **7**, 820–832 (2016).
57. Y. H. Jin *et al.*, Streamlined procedure for gene knockouts using all-in-one adenoviral CRISPR-Cas9. *Sci. Rep.* **9**, 277 (2019).
58. T. Matsu-Ura, M. Baek, J. Kwon, C. Hong, Efficient gene editing in Neurospora crassa with CRISPR technology. *Fungal Biol. Biotechnol.* **2**, 4 (2015).
59. B. Kim *et al.*, Multiplexed CRISPR-Cas9 system in a single adeno-associated virus to simultaneously knock out redundant clock genes. *Sci. Rep.* **11**, 2575 (2021).
60. C. H. Gabriel *et al.*, Live-cell imaging of circadian clock protein dynamics in CRISPR-generated knock-in cells. *Nat. Commun.* **12**, 3796 (2021).
61. M. Putker *et al.*, CRYPTOCHROMES confer robustness, not rhythmicity, to circadian timekeeping. *EMBO J.* **40**, e106745 (2021).
62. H. Flotow *et al.*, Phosphate groups as substrate determinants for casein kinase I action. *J. Biol. Chem.* **265**, 14264–14269 (1990).
63. A. Venerando, M. Ruzzene, L. A. Pinna, Casein kinase: The triple meaning of a misnomer. *Biochem. J.* **460**, 141–156 (2014).
64. R. Narasimamurthy, D. M. Virshup, The phosphorylation switch that regulates ticking of the circadian clock. *Mol. Cell* **81**, 1133–1146 (2021).
65. Y. Shinohara *et al.*, Temperature-sensitive substrate and product binding underlie temperature-compensated phosphorylation in the clock. *Mol. Cell* **67**, 783–798.e20 (2017).